Zoomorphology (2014) 133:405–416
DOI 10.1007/s00435-014-0230-y

ORIGINAL PAPER

Ultrastructural organization of lantern shark (*Etmopterus spinax* Linnaeus, 1758) photophores

Marie Renwart · Jérôme Delroisse · Julien M. Claes · Jérôme Mallefet

Received: 24 December 2013 / Revised: 11 March 2014 / Accepted: 15 March 2014 / Published online: 2 April 2014

Abstract *Etmopterus spinax* Linnaeus, 1758 is a deep-sea lantern shark that emits blue light thanks to thousands of tiny cup-shaped organs made of a pigmented sheath enclosing light-emitting cells topped by an iris-like structure and a lens. In this study, we investigate the ultrastructure of these photophores in order to improve our understanding of the light emission process. The presence of a novel layer, a putative reflector upholstering the pigmented sheath, is highlighted. The intracellular organization of the photocytes is addressed. They appear as regionalized cells: their basal area is occupied by an ovoid nucleus, their medial area is highly vesiculated and their apical area, oriented toward the photophore center, displays small granular inclusions. We hypothesize this granular area to be the intracellular site of photogenesis in *E. spinax*, as it is also the most fluorescent part of the photocyte.

Keywords Bioluminescence · Shark · Electron microscopy · Photocyte · Microsource

Communicated by A. Schmidt-Rhaesa.

M. Renwart (✉) · J. M. Claes · J. Mallefet
Laboratory of Marine Biology, Earth and Life Institute, Catholic University of Louvain (UCL), Place Croix du Sud 3, bt L7.06.04, 1348 Louvain-la-Neuve, Belgium
e-mail: marie.renwart@uclouvain.be

J. Delroisse
Biology of Marine Organisms and Biomimetics, University of Mons (UMONS), Avenue du Champ de Mars 6, 7000 Mons, Belgium

Introduction

In the deep ocean, most taxa have bioluminescent members that display a wide range of mechanisms to emit light and take advantage of this particular interaction tool (Haddock et al. 2010). The organ involved in this chemical process is called photophore but this generic term includes many different structural organizations (Hastings and Morin 1991). A luminescent unit can be as simple as one unique light-emitting cell, the photocyte, or shows a much more complex arrangement with numerous photocytes grouped in the center of an organ—the photophore *stricto senso*—and surrounded by various structures that enhance the light emission effectiveness, including protective pigmented layers, reflectors, focusing lenses and selective filters. In luminous symbiotic organisms (mainly some teleosts and cephalopods), photophores are specific structures containing luminous bacteria. In these bacterial photophores, the light reaching the outside can be controlled by a removable shutter or by physiological regulation (Herring 1982; Tong et al. 2009). Photophores also greatly differ in size, number and location: the teleosts *Photoblepharon palpebratus* Boddaert, 1781 and *Anomalops katoptron* Bleeker, 1856 display only two large suborbital symbiotic photophores of approximately 10 mm length (Haneda and Tsuji 1971); most euphausiid species bear ten photophores ranging from 0.1 to 0.6 mm in diameter (Herring and Locket 1978), while dalatiid sharks have thousands of 0.05-mm ventral photophores (Claes and Mallefet 2009).

Investigating the fine anatomy of photophores is a key step in the understanding of the light-emitting process and allows linking function with morphology (Strum 1969a, b). The ultrastructure of photophores has been described in various luminous species, and the knowledge of the photocyte's intracellular organization provided a better

understanding of the mechanism of bioluminescence. Microsources are the intracellular structures responsible of the photogenesis. They are as diverse in their forms and operating modes as the photophores themselves and often difficult to identify with certainty. In dinoflagellates, microsources, called *scintillons*, are small organelles protruding in a low-pH vacuole. An action potential along the membrane of the vacuole triggers the light by creating a protons flux toward the scintillon that activates the luciferase and releases the luciferin, the two components of the chemical reaction (Fritz et al. 1990). Coelenterates microsources, termed *lumisomes,* are vacuoles that are supposed to contain all the molecules of the light-emitting reaction, as only the addition of calcium ions is needed to produce light (Anderson and Cormier 1973). In adult fireflies, microsources refer to vesicles containing dense inclusions and microtubules. These vesicles share the features of peroxisomes and were found to show a catalase activity possibly related to light emission (Hanna et al. 1976). The *photosomes* of the Polynoidae are tridimensional tubules of endoplasmic reticulum that form a paracrystaline network bearing the protein responsible for the light emission, the polynoidin. An action potential releases oxygen radicals that activate this protein (Bassot and Nicolas 1987). Osteichthyes and Chondrichthyes are the only vertebrates known to be luminous. The ultrastructure of photocytes in Chondrichthyans remains to be studied in detail. In midshipman fish *Porichthys spp.*, the cytoplasm of the photocytes contains numerous vacuoles that tend to coalesce during the light emission, which suggest their involvement in the bioluminescent process (Anctil 1979a, b).

In Chondrichthyes, all Dalatiidae (kitefin sharks) and Etmopteridae (lantern sharks), which currently represent 56 species, 46 etmopterids and 10 dalatiids, have been assumed to be luminous (Ebert et al. 2013); eleven out of the twelve genera listed in these shark families have been documented to bear photophores (Claes and Mallefet 2009). Ohshima (1911) studied the structure of photophores in two etmopterid species (*Etmopterus lucifer* Jordan and Snyder, 1902 and *E. pusillus* Lowe, 1839) and found that the cup-shaped organ is composed of photocytes surrounded by pigmented cells, which form a pigmented sheath and iris-like structure, and topped by lens cells. Studies on the ontogeny of photophores in *E. spinax* Linnaeus, 1758 (Claes and Mallefet 2008) support the aforementioned results.

The purpose of this paper is to investigate the ultrastructure of *E. spinax* photophores in order to describe their different structural components with an emphasis on the intracellular organization of the photocytes. This first ultrastructural description is essential to improve our understanding of the light emission process occurring in these structures.

Materials and methods

Shark tissue collection

Specimens of *E. spinax* were caught by longlines in Norway (Raunefjord—60°15.908 N; 05°07.778 O) during two field missions in November 2012 and March 2013. Sharks were killed according to the local rules for experimental fish care. Fresh skin patches with photophores were dissected and fixed in a solution of either glutaraldehyde (3 % glutaraldehyde, 0.1 M sodium cacodylate, 0.27 M sodium chloride; pH 7.8) or formaldehyde (4 % formaldehyde, 0.052 M sodium phosphate monobasic, 0.082 M sodium phosphate dibasic; pH 8.4) during at least three hours. Skin patches were rinsed either in a cacodylate buffer (glutaraldehyde-fixed patches; 0.2 M sodium cacodylate, 0.31 M sodium chloride; pH 7.8) or in a phosphate buffer (formaldehyde-fixed patches; 0.081 M sodium phosphate dibasic, 1.37 M sodium chloride, 0.015 M potassium phosphate monobasic, 0.027 M potassium chloride, 0.25 % sodium azide; pH 8.4) and stored in the corresponding solutions. Glutaraldehyde-fixed patches were used for transmission electron microscopy (TEM) while formaldehyde-fixed patches were used for epifluorescence microscopy.

Transmission electron microscopy

Decalcification and post-fixation

Skin patches were immersed in a decalcifying solution (OsteoRAL R fast decalcifier, RAL diagnostics) for 10 days at room temperature with a continuous agitation (the solution was renewed every 2 days to avoid calcium saturation) in order to get rid of the elongated skin denticles that could jeopardize the sectioning process. Samples were then post-fixed in osmium tetroxide (1 % osmium tetroxide, 0.1 M sodium cacodylate, 0.27 M sodium chloride; pH 7.8) during 45 min and then progressively dehydrated in a graded ethanol series.

Embedding

Skin patches were embedded in a Spurr's resin [10 g ERL 4206 resin, 6 g DER 736 resin, 26 g nonenyl succinic anhydride, 0.4 g dimethylaminoethanol]. After one night of continuous agitation at room temperature, the resin solution was heated at 70 °C for 24 h to trigger polymerization.

Sections and contrast

Thin sections of 90–110 nm were obtained using an ultramicrotome (Leica Ultracut UCT—Leica Microsystems) and placed on copper grids. Sections were first contrasted in uranyl acetate [0.18 M uranyl acetate solution:ethanol (2:1)] during 45 min and secondly in lead citrate [0.08 M lead nitrate, 0.12 M sodium citrate, 0.16 M sodium hydroxide] during 4 min. After drying, sections were ready to be observed in a transmission electron microscope (Zeiss Leo 906E) where micrographs were taken. A 3D modeling of the structural components of the photophore was finally performed using the software Blender (Blender Foundation, Netherlands, software version 2.68).

Quantitative data

Areas of structures (i.e., lens, photocytes, pigments, photocyte vesicles and apical cells) were measured on the micrographs using Image J (National Institutes of Health, USA, software version 1.46r). These structures were assimilated to spherical elements with circular section, and their mean diameters with a standard error on the mean were post-calculated based on the measured areas. To measure the areas of the photocyte granules, the *watershed* option of Image J was first run to distinguish each individual granule from each other's. The *particle analysis* option was then applied to calculate the area of each granule, and one mean diameter was calculated per photocyte. The number of photocytes (N_{phot}) present in a photophore was estimated from selected photophore micrographs (those displaying at least two entire photocytes i.e., photocytes displaying their granular area in addition to their vesicular area and/or their nucleus, which indicate the section to pass through the photophore center), using the following formula:

$$N_{phot} = \left(\frac{A_{phot}}{A_{tot}}\right)^{\frac{3}{2}}$$

where A_{phot} is the area of an entire photocyte and A_{tot} is the whole area occupied by photocytes.

Fluorescence observations

Skin patches fixed with formaldehyde were decalcified and embedded as described before. Semi-thin sections of 600 nm were obtained using the ultramicrotome, put on a slide and directly observed with a fluorescence microscope (Leitz Diaplan). No post-fixation and contrast steps were applied.

Results

Structure of the photophore

The 3D modeling (Fig. 1) shows an overview of the structures constituting the photophore: a hemispherical cup-shaped layer of pigmented cells, the pigmented sheath, that encloses the other components surmounted by different cell types (I and II) that make the transition to the lens, placed in the apical region of the photophore (Fig. 1a). As the pigmented sheath is removed, a previously undescribed layer, the reticulated layer, is highlighted (Fig. 1b). Inside the reticulated layer, the light-emitting photocytes show a particular orientation toward the center of the photophore (Fig. 1c, d). In cross-section (Fig. 2), the pigmented sheath and the reticulated layer form an arch-like structure and photocytes appear as ovoid cells packed against each other, leaving few intracellular spaces. On each side of the photocytes, some pigmented cells form the iris-like structure. Number of photocytes per photophore (N_{phot}) was estimated to range from 5.22 to 18.66 (mean number = 13.16 ± 0.76, $N = 18$).

Pigmented sheath and iris-like structure

The pigmented cells can be either elongated and piled on each other as a heap of leaves in the pigmented sheath (Fig. 3a, b) or branched and spread on each side of the photophore in the iris-like structure (Fig. 3a, c). Inside the pigmented cells, dark pigments are densely packed to form numerous oval melanosome-like organelles (diameter of 0.39 ± 0.01 μm, $N = 100$).

Reticulated layer

This layer enclosed the photocytes and upholsters the inner face of the pigmented sheath. It is packed of thin cells with a flattened nucleus pushed against the cell wall and a lumen filled with a reticulated matrix (Fig. 4a). This three dimensional web is composed of fibrous material forming polygonal boxes that appear empty on the micrographs (Fig. 4b).

Photocytes

Photocytes (diameter of 15.46 ± 0.51 μm, $N = 34$) are regionalized cells grouped in the center of the photophore just above the reticulated layer (Fig. 5a). Their spherical nucleus, which presents deep cytoplasm protrusions (Fig. 5b), is usually located in their basal part and adjoins

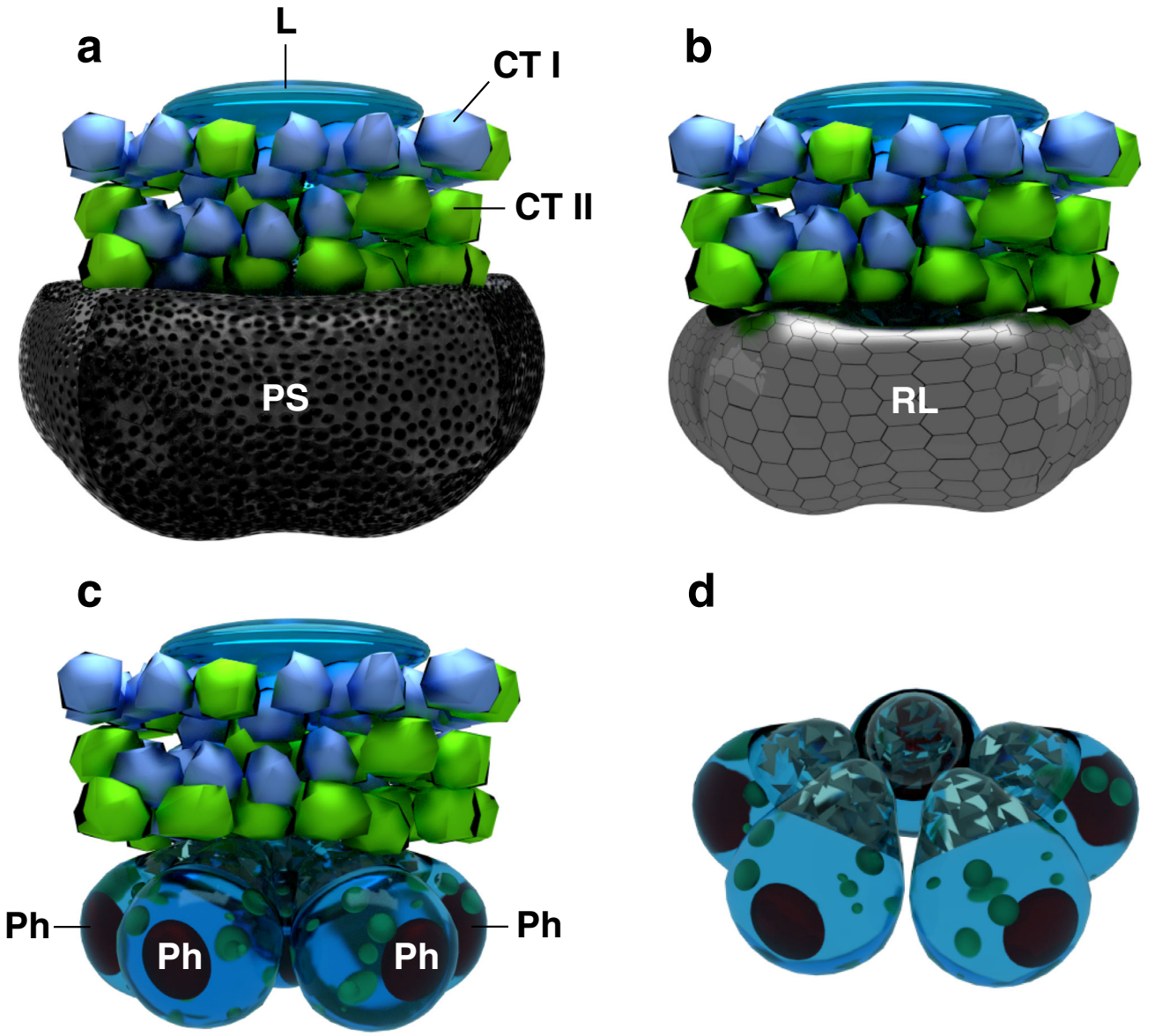

Fig. 1 3D modeling of the photophore. **a** Entire photophore with photocytes enclosed in the pigmented sheath (*PS*). **b** Reticulated layer (*RL*) revealed by pigmented sheath removal. **c** Photocytes (*Ph*) revealed by reticulated layer removal. **d** Photocytes isolated from other photophore components, revealing their particular orientation. *CT I* cellular type I, *CT II* cellular type II, *L* lens

a highly vesiculated region that will be further referred as the "vesicular area." In this intermediate zone, vesicles are numerous and can be separated into two types: ovoid (diameter of 2.12 ± 0.13 µm, $N = 36$) and polygonal vesicles (diameter of 0.49 ± 0.02 µm, $N = 100$), which are more numerous. The apical region of the photocyte is completely filled with granular inclusions (diameter of 0.38 ± 0.01 µm, $N = 44$) irregularly shaped and dense to electrons; it will further be referred as the "granular area." By contrast, the lumen surrounding the granular inclusions appears white, revealing no electron absorbance there (Fig. 5f). This area is not surrounded by a membrane although it forms a distinct part of the cytoplasm. The granules present in this region can also be found in smaller number in the vesicular area, packed between the vesicles. In this sense, both areas seem to be a continuum (Fig. 5d, e). Interestingly, the areas of the photocytes are not oriented randomly: The granular area of a photocyte is always oriented toward the center of the photophore (Figs. 2b, 3a, 6). This typical orientation is also visible in fluorescence microscopy as the granular area presents the highest fluorescence intensity (Fig. 7).

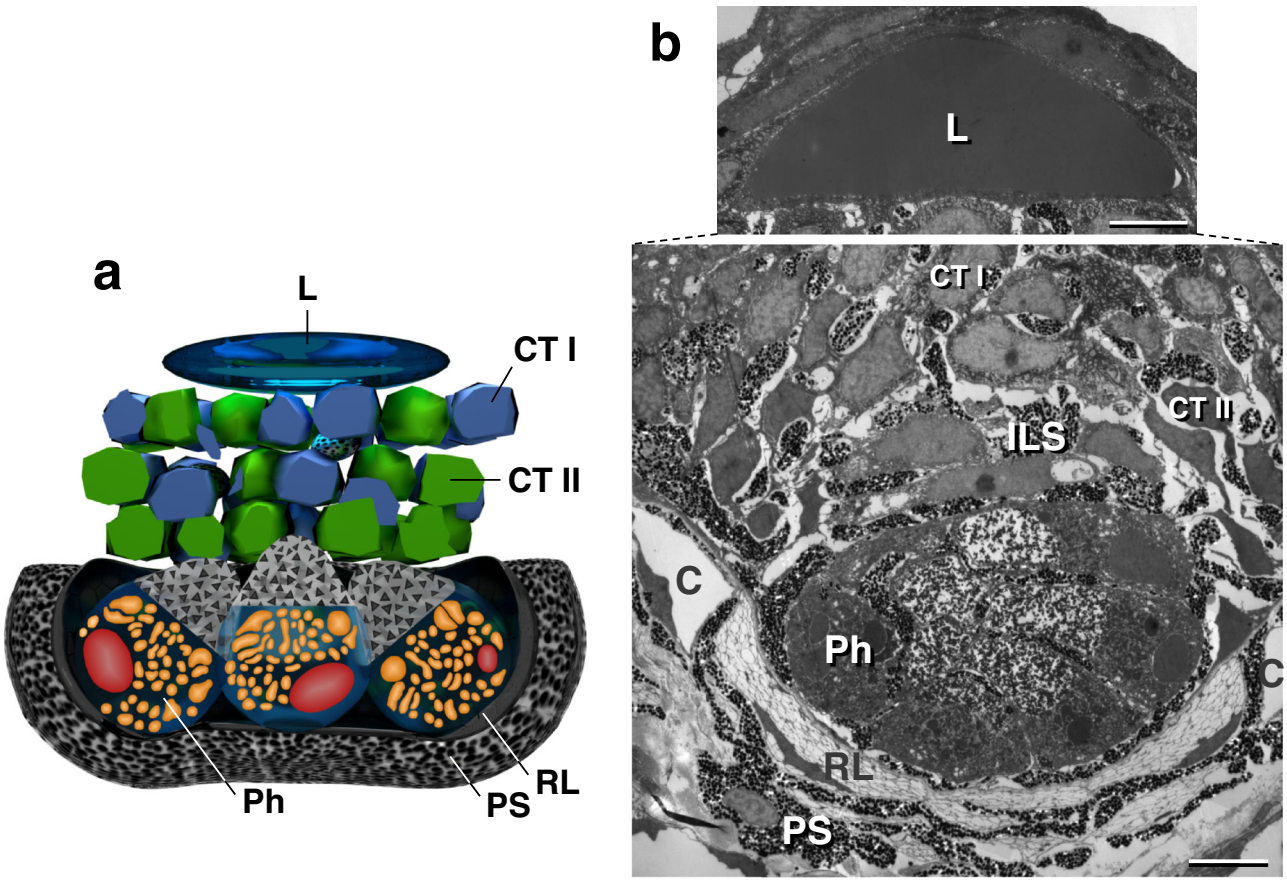

Fig. 2 Cross-sections of a photophore. **a** 3D modeling of a cross-section in a photophore. **b** Corresponding micrograph cross-section in a photophore. *C* capillary, *CT I* cellular type I, *CT II* cellular type II, *ILS* iris-like structure, *L* lens, *Ph* photocyte, *PS* pigmented sheath, *RL* reticulated layer. *Scale bar* 10 µm

Apical structures

Above the photocytes are located different cell types that make the transition between the photogenic and lens cells. In the first cellular type (diameter of 10.79 ± 0.27 µm, $N = 32$), the nucleus, located in the center of the cell, is surrounded by a fibrous material that constitutes a tridimensional web filling the whole cytoplasm (Fig. 8a, b). Those cells are preferentially located near the lens (Fig. 2b). Only the nucleus of the second cellular type—usually observed closer to the photocytes (Fig. 2b)—can be observed (Fig. 8c). For this reason, no quantitative data were taken. The lens (diameter of 27.7 ± 1.2 µm, $N = 20$) is composed of one or sometimes two cells situated at the apical end of the photophore. These cells are bigger than any other cells in the photophore and present a typical convex shape (Fig. 2b). The nucleus of the cell is pushed against the cell membrane, as the cytoplasm is entirely filled with a vacuole containing a homogeneous substance moderately dense to electron.

Discussion

Previous studies, using optical microscopy, revealed a simple organization of the etmopterid light-emitting organ: a cup-shaped hemisphere composed of a protective layer of pigmented cells, an iris-like structure, a few photocytes and a lens (Johann 1899; Ohshima 1911; Claes and Mallefet 2008). Using the TEM technique, we were able to investigate the ultrastructure of photophores of the lantern shark *Etmopterus spinax* and the presence of an undescribed layer as well as various intracellular components have been highlighted.

Fishes show a great diversity in the morphology and operating mode of their photogenic structures. The suborbital photophores of the teleosts *Photoblepharon spp*. and *Anomalops spp*. are large elliptical organs containing tubules full of luminous bacteria measuring from 2 to 3.3 µm long and identifiable on electron micrographs (Haneda and Tsuji 1971). So far, no bacterial symbionts have been reported in luminous sharks, and our results did

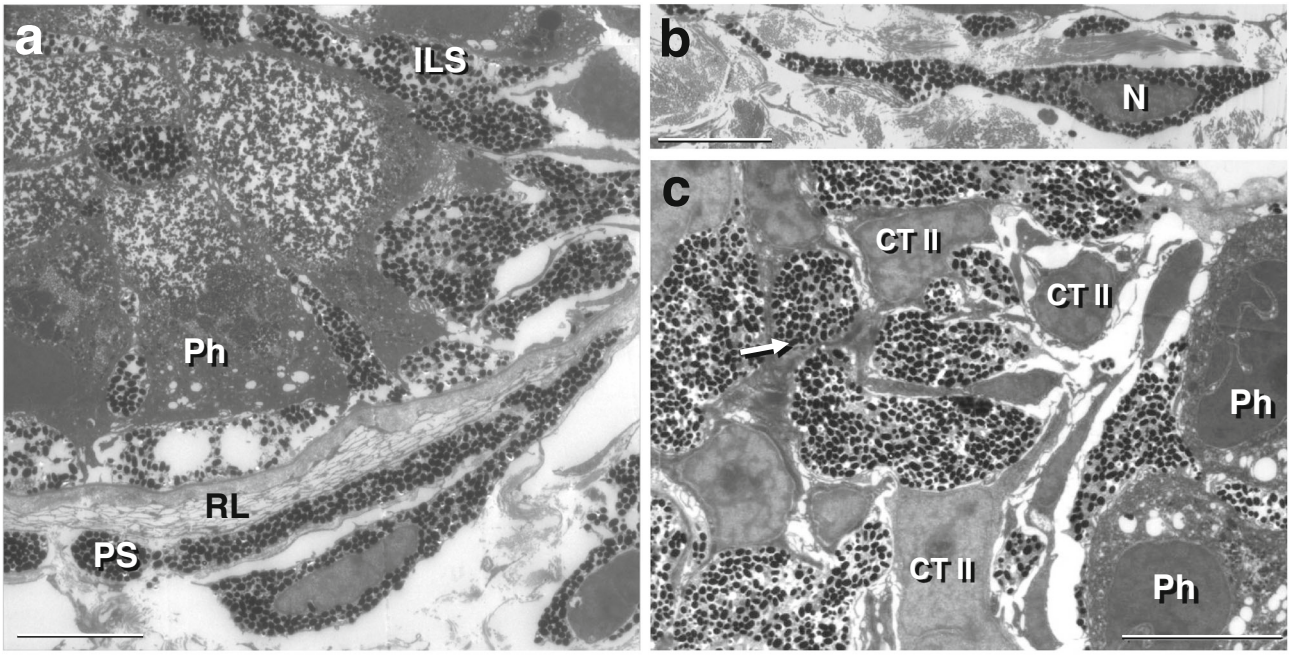

Fig. 3 Pigmented cell morphologies. **a** Photophore cross-section showing the pigmented sheath (*PS*) and the iris-like structure (*ILS*). **b** Typical shape of the pigmented cells when located in the pigmented sheath. **c** Typical shape of the pigmented cells when located in the iris-like structure. *Arrow* shows a pigment organelle. *CT II* cellular type II, *N* nucleus, *Ph* photocyte, *RL* reticulated layer. *Scale bar* 10 µm

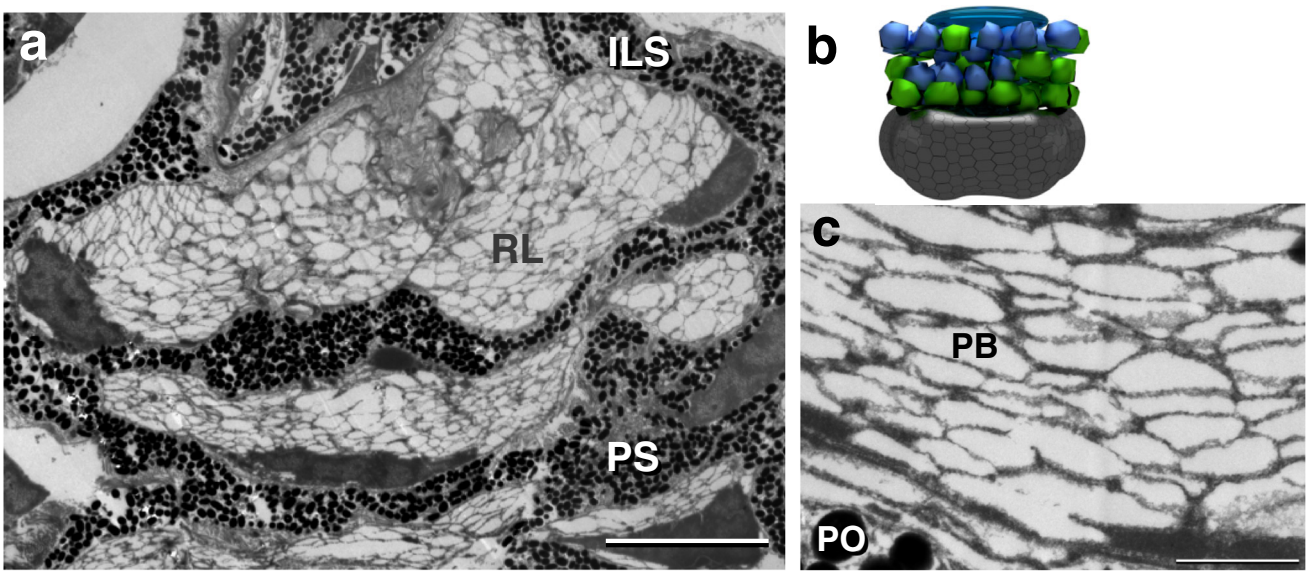

Fig. 4 Reticulated layer. **a** Photophore cross-section located before the photocytes and showing the reticulated layer (*RL*). *Scale bar* 10 µm. **b** The corresponding 3D modeling. **c** Magnification of the reticulated matrix. *ILS* iris-like structure, *PO* pigment organelle, *PB* polygonal box, *PS* pigmented sheath. *Scale bar* 1 µm

not reveal the presence of bacteria inside the photocytes of *E. spinax*. Intrinsic luminescence, on the opposite, is the light produced by chemicals within an organism's intrinsic tissue and not by symbionts (Haddock et al. 2010). In most intrinsic photogenic structures, the luminous material

Fig. 5 Photocyte zonation. **a** Typical regionalization of the photocyte ▶ with the nucleus (*N*), the vesicular area (*VA*) and the granular area (*GA*). **b** Nucleus with its cytoplasmic protrusions (*arrow*). **c** Vesicular area showing numerous homogenous gray dense vesicles (*V*). **d** and **e** Transition between the vesicular and the granular areas showing a continuum between both. **f** Granular area with congregated granular inclusions (*GI*). Non-captioned *scale bars*, 2 µm

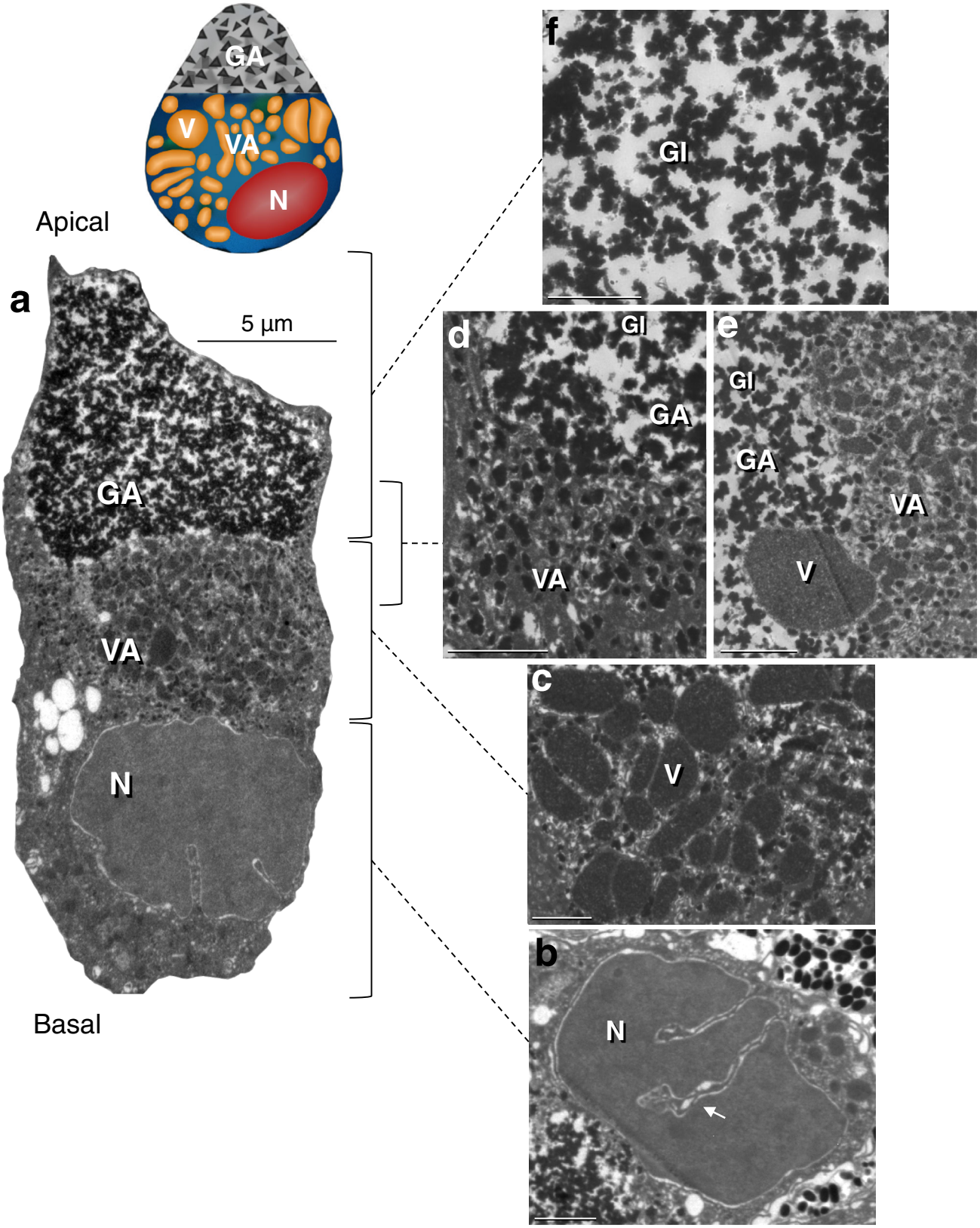
GA
V
VA
N
Apical
a
5 µm
GA
VA
N
Basal
f
Gl
d
Gl
GA
VA
e
Gl
GA
VA
V
c
V
b
N

remains within the photocytes, but secretory luminescence can also be observed. In sharks, this particular light emission mechanism is reported for *Euprotomicroides zantedeschia* Hulley and Penrith, 1966, which has been hypothesized to eject luminescent secretion from the abdominal pouch (Munk and Jorgensen 1988). In teleosts, secretory luminescence has been studied in *Gonostoma elongatum* Günther, 1878. These particular photogenic structures are very different from what we observed in *E. spinax* photophores (Fig. 9), which did not show any excretory structure.

Shark photocytes are generally encircled by pigmented cells, in both etmopterid and dalatiid species (Claes and Mallefet 2009), and this structural characteristic is also present in Osteichthyes (Fig. 9). In *E. spinax*, we showed that pigmented cells present different morphologies according to their role in the light emission process. Flat and elongated pigmented cells form the sheath that prevents light dispersion toward the dermis and underlying muscles, while branched pigmented cells form an iris-like structure that mechanically control the light emission. Ohshima (1911) studied the iris-like structure of etmopterid and found that pigmented cells display "pseudopodia-like projections" in three directions that decrease the light reaching the outside, which is supported by our results (Fig. 3a, c). The iris-like structure has been shown to open when the photophore is stimulated by adequate hormones, resulting in an increase in light intensity by retraction of the "pseudopodia-like projections" (Claes and Mallefet 2010).

To efficiently counterilluminate, pelagic organisms have to produce a ventral glow matching the angular distribution, intensity and spectrum of residual downwelling light (Denton et al. 1972). As a consequence, most counterilluminating teleosts and cephalopods have developed accessory structures such as specialized filters

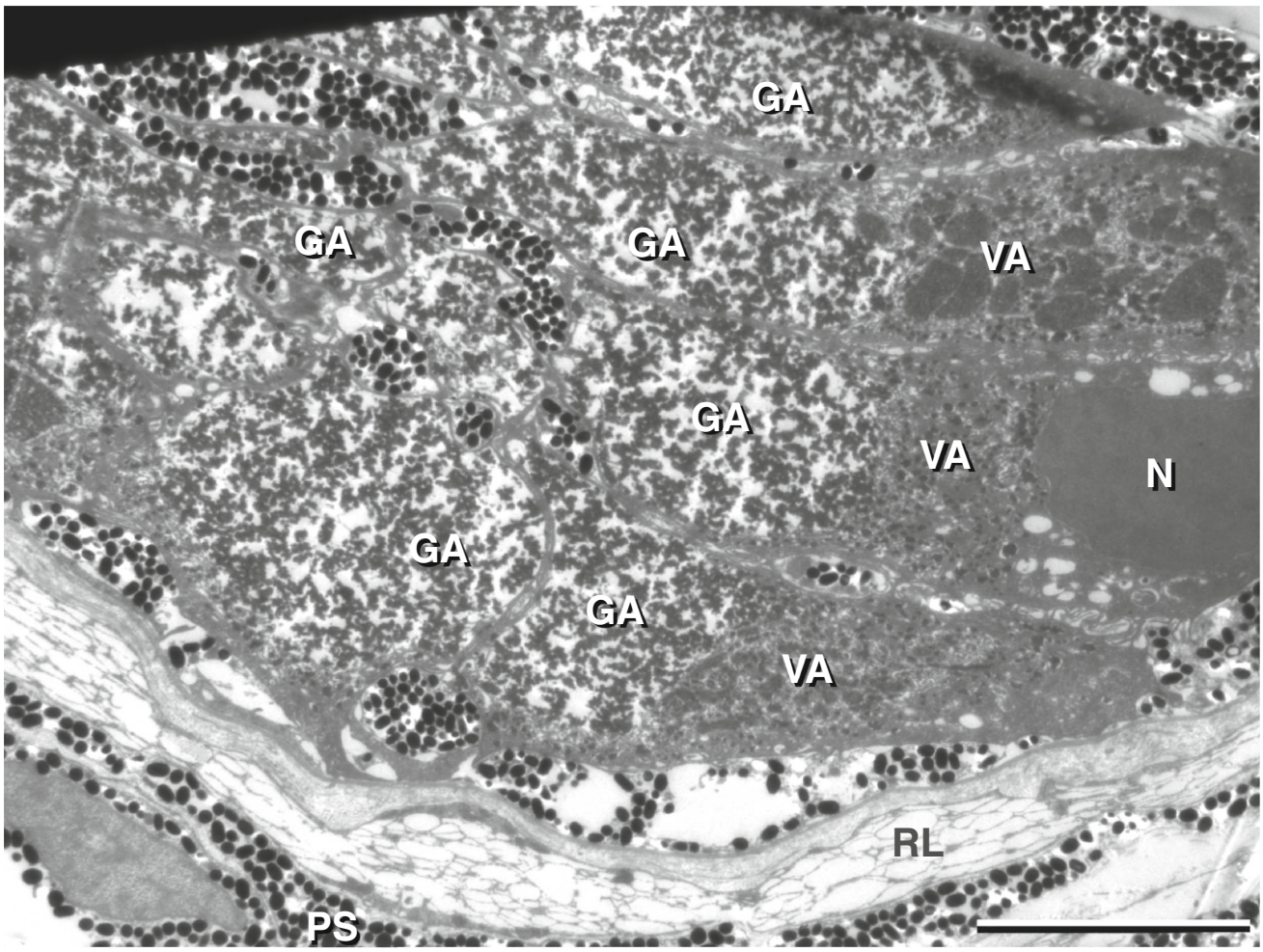

Fig. 6 Group of photocytes showing the characteristic orientation of the granular areas (GA). *N* nucleus, *PS* pigmented sheath, *RL* reticulated layer, *VA* vesicular area. *Scale bar* 10 μm

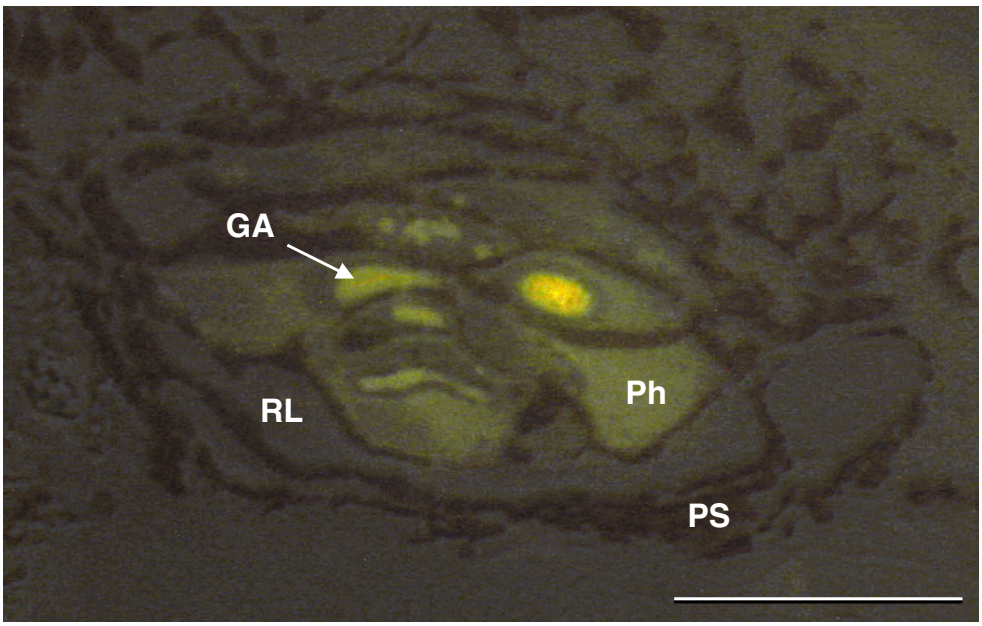

Fig. 7 Superimposition of two pictures of a 600-nm photophore cross-section: a fluorescent picture showing the autofluorescence of the photocytes and a white light picture showing the delimitations of the photocytes. *Ph* photocyte, *PS* pigmented sheath, *RL* reticulated layer, *GA* granular area. *Scale bar* 50 µm

and reflectors to finely tune the physical characteristics of their luminescence (Nicol 1957; Denton et al. 1972, 1985; Harper and Case 1999; Jones and Nishiguchi 2004). These optical structures, on the other hand, are considered to be absent in shark photophores (Iwai 1960; Herring and Morin 1978), which is surprising since these organs can also be used in counterillumination as it was recently confirmed in *E. spinax* (Claes et al. 2010a). However, given the spatial organization and general morphology of the reticulated layer (Figs. 1, 2, 4), which are similar to previously described reflective structures (Denton 1970; Fishelson et al. 2005), we hypothesize this layer to fulfill the function of a reflector in *E. spinax* photophores. Indeed, the cells of the reticulated layer contain a reticulated matrix of polygonal boxes (Fig. 4b) that appear similar to those observed in others species such as the cardinal fish *Siphamia cephalotes* Castelnau, 1875 (Fishelson et al. 2005) or the midshipman fish *Porichthys notatus* Girard, 1854, although reflector cells of the latter appear more needle shaped (Strum 1969a, b). The presence of the reticulated layer in dalatiid species still remains to be confirmed. The polygonal boxes in *E. spinax* might have enclosed crystals with reflective properties. Reflector crystals usually refer to guanine (Denton 1970; Denton et al. 1985; Fishelson et al. 2005), which unfortunately have the property to solubilize when stained with uranyl acetate and lead citrate (Strum 1969a, b), a method used in this study. Attesting the reflective role of the reticulated matrix would therefore require unstained thin sections in order to study the reflective properties and characteristics (thickness and orientation) of crystals.

The lens is a major component of fish photophores with internal light events. The typical convex shape of the lens covering *E. spinax* photophores (Fig. 2b) is perfectly designed to focus the light emitted outside. The role of the two cell types located between the photocytes and the lens is more difficult to assess. The cellular type I, which contains fibrous material and are often closely associated with the lens (Figs. 2b, 8a, b), probably ensure the stability of the lens even though they could also be involved in the control of the light emission. From the cellular type II, only the nucleus is still visible in the sections (Fig. 8c). For this reason, hypothesizing its function based on the morphology is impossible. Yet an involvement in the light emission control can also be suggested here. Claes et al. (2011) demonstrated the presence of γ-aminobutyric acid (GABA) in the cells surrounding photocytes and in the epidermal cells and argued for GABAergic modulation of the light emission in *E. spinax*. A closer examination of these cells using immunocytological techniques would be necessary to reveal the presence of GABA.

We found between 5 and 18 photocytes per photophore in *E. spinax*, which is slightly higher than previous estimation on this species (4–6, Johann 1899), but close to what was observed in two other etmopterid species, *E. lucifer* and *E. pusillus* (about 14, Ohshima 1911). Although the higher number found in this study regarding *E. spinax* might be linked to intraspecific difference,

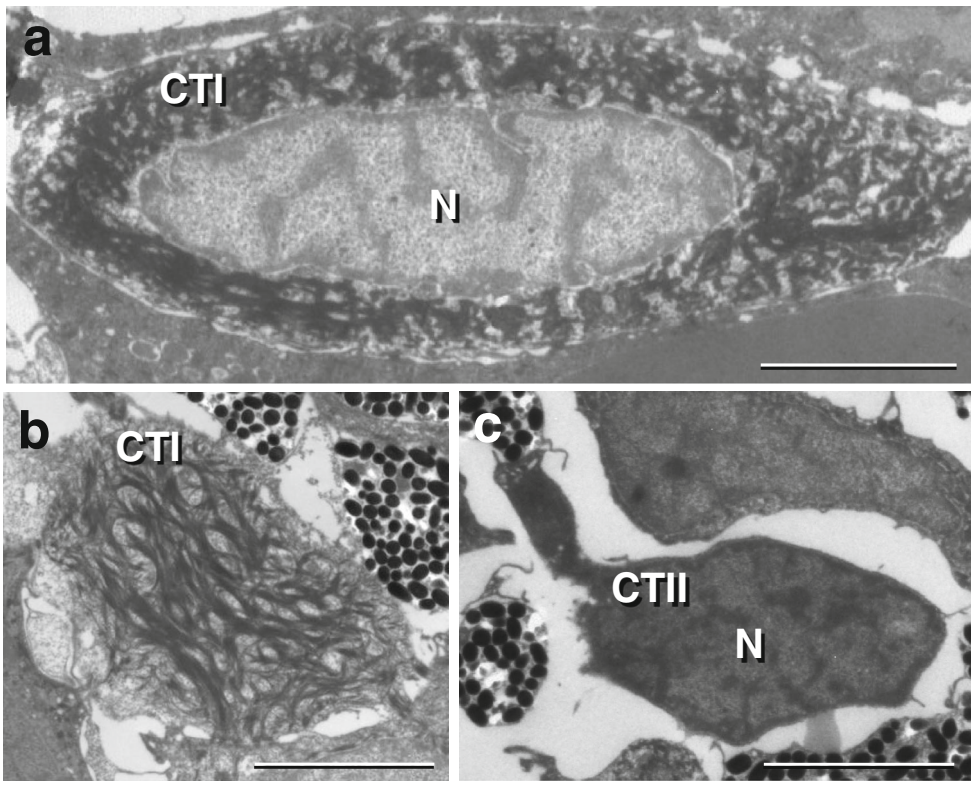

Fig. 8 Cellular types I and II. **a** Typical nucleus (*N*) location in the center of the cellular type I (*CTI*). **b** Fibrous material filling the cytoplasm of the cellular type I. **c** Nucleus of the cellular type II (*CTII*). *Scale bar* 5 μm

it might also be linked to our TEM-based three dimensional estimation method, which provides higher but more accurate values than simple two-dimensional countings. The main structural difference regarding etmopterid and dalatiid photophores lies in the presence of a single photocyte in this latest (Fig. 9), the ultrastructure of which remains to be studied. Interestingly, however, embryos of *E. spinax* also display photophores with single photocytes (Claes and Mallefet 2008; Claes et al. 2010b), a feature among others suggesting a unique origin of luminescence capability in sharks (Claes et al. 2012).

E. spinax photocyte ultrastructure revealed the presence of an apical area full of small granular inclusions i.e., the granular area, which is always oriented toward the center of the photophore, below the lens (Figs. 2b, 3a, 6). This feature has been observed in *P. notatus* (Strum 1969a, b). We suggest that such a physical conformation, which is not random, aims to optimize the amount of light captured by the lens. By superimposing a picture showing the autofluorescence of the photocytes with the same picture in white light, we observed that the granular area corresponds to the most intense fluorescent part of the photocyte (Fig. 7). In some cases (e.g., in the cephalopod *Vampyroteuthis infernalis* Chun, 1903; Robison et al. 2003), bioluminescent compounds are autofluorescent and this fluorescence helps to locate the bioluminescence site (Bassot and Bilbaut 1977; Sweeney 1980). The granular area likely also corresponds to the previously described "fluorescent vesicle" (Claes and Mallefet 2008; Claes et al. 2010b). It must be pointed out that no membrane surrounding this area was observed, and therefore, it does not form a delimitated vesicle *per se*. Because the apparition of this fluorescent area has been correlated with the functionality of the photophore in *E. spinax* embryos (Claes and Mallefet 2008), we assume the granular area to represent the site of photogenesis and hence the granular inclusions to be the microsources of *E. spinax* photophores. The role of the vesicles, located in the vesicular area, is still unknown. We cannot rule out their involvement in the bioluminescent process possibly by storing or releasing one of the components of the chemiluminescent reaction.

In conclusion, this study provides evidence of an intrinsic bioluminescence with no excretory activity in *E. spinax* photophores. In addition, it reveals the presence of a novel reflector-like layer and putative microsources in the apical granular area of the photocytes. Future work will

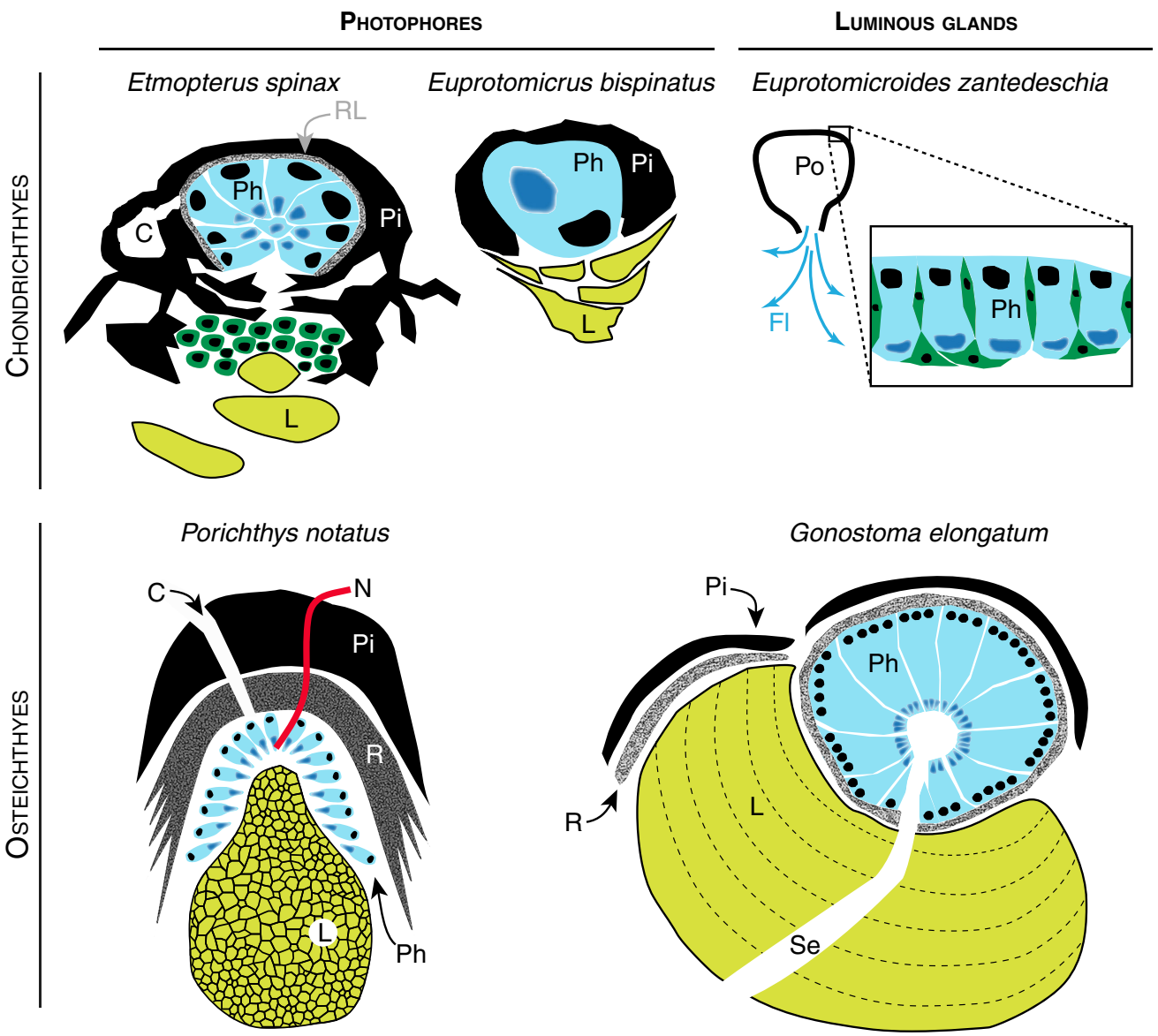

Fig. 9 Intrinsic ventral photophores of fishes. A similar *color highlights* analogous structures. Unlabeled cells in *E. spinax* and *E. zantedeschia* are cells closely associated with photogenic tissue whose function is uncertain. *C* capillary, *Fl* excreted luminous fluid, *L* lens, *N* nerve, *Ph* photocyte, *Pi* pigmented cells, *Po* pouch with secretory photogenic epithelium, *RL* reticulated layer, *R* reflector, *Se* secretory duct

attempt to characterize the morphological changes occurring within the photocytes during the light emission process.

Acknowledgments This work was supported by a grant from the Fonds de la Recherche Scientifique (FRS-FNRS, Belgium) to M. R. and a Grant from the Fonds de la Recherche Fondamentale Collective (FRFC—2.4525.12). J. D., J. M. C. and J. M. are, respectively, Research Fellow, Postdoctoral Researcher and Research Associate of the FRS-FNRS. We would like to thank T. Stassin for the design of the 3D modeling, A. Aadnesen, manager of the Espegrend Marine Biological Station (University of Bergen, Norway) where animals were kept and T. Sorlie for the help during field collections. This paper is a contribution to the Biodiversity Research Center (BDIV) and to the Centre Interuniversitaire de Biologie Marine (CIBIM).

References

Anctil M (1979a) Ultrastructural correlates of luminescence in *Porichthys* photophores. I. Effects of spinal cord stimulation and exogenous noradrenaline. Rev Can Biol 38:67–80

Anctil M (1979b) Ultrastructural correlates of luminescence in *Porichthys* photophores. II. Effects of metabolic inhibitors. Rev Can Biol 38:81–96

Anderson JM, Cormier MJ (1973) Lumisomes, the cellular site of bioluminescence in coelenterates. J Biol Chem 248:2937–2943

Bassot J-M, Bilbaut A (1977) Bioluminescence des élytres d'*Acholoe*. IV. Luminescence et fluorescence des photosomes. Biol Cellulaire 28:163–168

Bassot J-M, Nicolas G (1987) An optional dyadic junctional complex revealed by fast-freeze fixation in the bioluminescent system of the scale worm. J Cell Biol 105:2245–2256

Claes JM, Mallefet J (2008) Early development of bioluminescence suggests camouflage by counter-illumination in the velvet belly lantern shark *Etmopterus spinax* (Squaloidea: Etmopteridae). J Fish Biol 73:1337–1350

Claes JM, Mallefet J (2009) Bioluminescence of sharks: first synthesis. In: Meyer-Rochow VB (ed) Bioluminescence in focus: a collection of illuminating essays. Research Signpost, Kerala, pp 51–65

Claes JM, Mallefet J (2010) The lantern shark's light switch: turning shallow water crypsis into midwater camouflage. Biol Lett 6:685–687

Claes JM, Aksnes DL, Mallefet J (2010a) Phantom hunter of the fjords: camouflage by counterillumination in a shark (*Etmopterus spinax*). J Exp Mar Biol Ecol 388:28–32

Claes JM, Krönström J, Holmgren S, Mallefet J (2010b) Nitric oxide in the control of luminescence from lantern shark (*Etmopterus spinax*) photophores. J Exp Biol 213:3005–3011

Claes JM, Krönström J, Holmgren S, Mallefet J (2011) GABA inhibition of luminescence from lantern shark (*Etmopterus spinax*) photophores. Com Biochem Physiol 153C:231–236

Claes JM, Ho HC, Mallefet J (2012) Control of luminescence from pygmy shark (*Squaliolus aliae*) photophores. J Exp Biol 215:1691–1699

Denton EJ (1970) Review lecture: on the organization of reflecting surfaces in some marine animals. Philos Trans R Soc Lond 258B:285–313

Denton EJ, Gilpin-Brown JB, Wright PG (1972) The angular distribution of the light produced by some mesopelagic fish in relation to their camouflage. Proc R Soc Lond 182B:145–158

Denton EJ, Herring PJ, Widder EA, Latz MF, Case JF (1985) The roles of filters in the photophores of oceanic animals and their relation to vision in the oceanic environment. Proc R Soc Lond 225B:63–97

Ebert DA, Fowler SL, Compagno LJ (2013) Sharks of the world: a fully illustrated guide. Wild Nature Press, Plymouth

Fishelson L, Gon O, Goren M (2005) The oral cavity and bioluminescent organs of the cardinal fish species *Siphamia permutata* and *S. cephalotes* (Perciformes, Apogonidae). Mar Biol 147:603–609

Fritz L, Morse D, Hastings JW (1990) The circadian bioluminescence rhythm of *Gonyaulax* is related to daily variations in the number of light-emitting organelles. J Cell Sci 95:321–328

Haddock SHD, Moline MA, Case JF (2010) Bioluminescence in the sea. Annu Rev Mar Sci 2:443–493

Haneda Y, Tsuji FI (1971) Light production in the luminous fishes *Photoblepharon* and *Anomalops* from the Banda Islans. Science 173:143–145

Hanna CH, Hopkins TA, Buc J (1976) Peroxisomes of the firefly lantern. J Ultrastruct Res 57:150–162

Harper RD, Case JF (1999) Disruptive counterillumination and its anti-predatory value in the plainfish midshipman *Porichthys notatus*. Mar Biol 134:529–540

Hastings JW, Morin JG (1991) Bioluminescence. In: Prosser CL (ed) Neural and integrative animal physiology. Wiley-Liss, New York, pp 131–170

Herring PJ (1982) Aspects of the bioluminescence of fishes. Oceanogr Mar Biol Ann Rev 20:415–470

Herring PJ, Locket NA (1978) The luminescence and photophores of euphausiid crustaceans. J Zool 186:431–462

Herring PJ, Morin JG (1978) Bioluminescence in fishes. In: Herring PJ (ed) Bioluminescence in action. Academic Press, London, pp 273–329

Iwai T (1960) Luminous organs of the deep-sea squaloid shark, *Centroscyllium ritteri* Jordan and Fowler. Pac Sci 14:51–54

Johann L (1899) Über eigenthümliche epitheliale Gebilde (Leuchtorgane) bei *Spinax niger*. Z Wiss Zool 66:136–160

Jones BW, Nishiguchi MK (2004) Counterillumination in the Hawaiian bobtail squid, *Euprymna scolopes* berry (Mollusca: Cephalopoda). Mar Biol 144:1151–1155

Munk O, Jorgensen JM (1988) Putatively luminous tissue in the abdominal pouch of a male dalatiine shark, *Euprotomicroides zantedeschia* Hulley and Penrith, 1966. Acta Zool 69:247–251

Nicol JA (1957) Observations on photophores and luminescence in the teleost *Porichthys*. Q J Microsc Sci 98:179–188

Ohshima H (1911) Some observations on the luminous organs of fishes. J Coll Sci Imp Univ Tokyo 27:1–25

Robison BH, Reisenbichler KR, Hunt JC, Haddock SHD (2003) Light production by the arm tips of the deep-sea cephalopod *Vampyroteuthis infernalis*. Biol Bull 205:102–109

Strum JM (1969a) Fine structure of the dermal luminescent organs, photophores, in the fish, *Porichthys notatus*. Anat Rec 164:433–462

Strum JM (1969b) Photophores of *Porichthys notatus*: ultrastructure of innervation. Anat Rec 164:463–478

Sweeney BM (1980) Intracellular source of bioluminescence. Int Rev Cytol 68:173–195

Tong D, Rozas NS, Oakley TH, Mitchell J, Colley NJ, McFall-Ngai MJ (2009) Evidence for light perception in a bioluminescent organ. Proc Natl Acad Sci USA 106:9836–9841